Available online at www.sciencedirect.com
SCIENCE DIRECT®
International Journal of Heat and Mass Transfer 47 (2004) 4031–4043
International Journal of HEAT and MASS TRANSFER
www.elsevier.com/locate/ijhmt

Experimental and theoretical investigation of reflux condensation in an inclined small diameter tube

S. Fiedler [a], H. Auracher [b,*]

[a] Degussa AG, VT-P, Rodenbacher Chaussee 4, Hanau 63457, Germany
[b] TU Berlin, Institut für Energietechnik, KT1, Marchstrasse 18, Berlin 10587, Germany

Received 31 December 2003; received in revised form 2 June 2004

Abstract

Heat transfer, flooding point and film thickness during reflux condensation of refrigerant R134a in an inclined small diameter tube (ID: 7 mm, length: 500 mm) are experimentally investigated. Also a physical model for laminar reflux condensation of a pure saturated vapour in an inclined small diameter tube is presented. The theoretical results for the film thickness and the heat transfer are compared with the experimental data. It is found that the inclination angle has a significant effect on the heat transfer coefficient and the flooding point. The calculated values for the film thickness and the mean heat transfer coefficient are in good agreement with the experimental data. The deviation is less than 15%.

1. Introduction

Compact plate heat exchangers are increasingly used for reflux condensation applications. In such condensers the hydraulic diameter of the flow channels formed between two plates is 5–10 mm, and the flow channels are inclined to the vertical. The fundamental mechanisms of heat and mass transfer as well as of two-phase flow in these small channels are not well understood. In this fundamental study reflux condensation of refrigerant R134a is investigated in an idealised single sub-channel of a compact condenser namely a small diameter inclined tube. The inner diameter of the test tube is 7 mm and its length is 500 mm.

Reflux condensation refers to the condensation process in which the vapour enters the condenser at the bottom and flows upward whilst the condensate flows downward countercurrently to the vapour due to gravity. Reflux condensation is limited by the phenomenon of flooding: there is a maximum vapour velocity above which at least part of the condensate will be carried upward rather than draining to the bottom. This limiting condition is referred to as the onset of flooding or the flooding point and the corresponding vapour velocity at this point is known as the flooding vapour velocity.

In case of reflux condensation flooding will be initiated at the vapour inlet. At this point the maximum gas velocity and the maximum liquid mass flow rate occur. Much of the experimental work on flooding has been undertaken at adiabatic conditions, typically the air-water combination in vertical tubes with relatively large tube diameters. However, flooding experiments under adiabatic conditions are not directly comparable with those under reflux condensation conditions.

Mouza et al. [1] obtained, for example, flooding data for a vertical and inclined 0.8 m long glass tube with an inner diameter of 7 mm using air and water. They compared their experimental data for the vertical tube with the data predicted by the well known Wallis correlation:

$$\left(w_g'^{+}\right)^{1/2} + C_1\left(w_l'^{+}\right)^{1/2} = C_2. \quad (1)$$

They found that the Wallis correlation agrees well with their experimental data for the vertical tube when

* Corresponding author. Tel.: +49-30-314-25710; fax: +49-30-314-21779.
E-mail addresses: stefan.fiedler@degussa.com (S. Fiedler), auracher@iet.tu-berlin.de (H. Auracher).

0017-9310/$ - see front matter © 2004 Elsevier Ltd. All rights reserved.
doi:10.1016/j.ijheatmasstransfer.2004.06.005

Nomenclature

A	cross-sectional area, m^2
C_1, C_2	constants in Eq. (1)
c	sound speed, m/s
c_p	specific heat at constant pressure, J/(kg K)
d	diameter, m
g	gravitational constant, m/s^2
Δh_v	specific enthalpy of vaporization, J/kg
L	length, m
$\dot{M}$	mass flow rate, kg/s
Nu	Nusselt number, dimensionless
$\dot{Q}$	total heat flow rate, W
R	radius, m
Re	Reynolds number, dimensionless
T	temperature, K
ΔT	temperature difference, K
Δt	time lag, s
w	velocity, m/s
w'	superficial velocity, m/s
x	coordinate, dimensionless
y	coordinate, dimensionless
Z	axial coordinate, dimensionless
z	coordinate, dimensionless

Greek symbols

α_m	mean heat transfer coefficient for entire tube surface, $W/(m^2 K)$
α_M	mean heat transfer coefficient for an infinitesimal ring of tube surface, $W/(m^2 K)$
β	inclination angle, °
δ	film thickness, m
η	dynamic viscosity, kg/(m s)
λ	thermal conductivity, W/(m K)
v	kinematic viscosity, m^2/s
ρ	density, kg/m^3
σ	surface tension, N/m
ϕ	peripheral angle, °
ϕ^*	peripheral angle of condensate layer, °
Ψ	dimensionless film thickness

Subscripts and superscripts

CL	condensate layer
CW	cooling water
cond	condensate
exp	experimental
g	gas, vapour
h	hydraulic
l	liquid, condensate
m	mean
n	according to Nusselt's film theory
S	saturation
theo	theoretical
W	wall
$^+$	dimensionless

the parameters C_1 and C_2 are both taken to be 1.0. The dimensionless superficial velocities are defined as follows:

$$w_g'^+ = w_g' \rho_g^{1/2} [g d(\rho_l - \rho_g)]^{-1/2}, \tag{2}$$

$$w_l'^+ = w_l' \rho_l^{1/2} [g d(\rho_l - \rho_g)]^{-1/2}. \tag{3}$$

A correlation that is often used in process industry to predict the flooding point in reflux condensers is the one proposed by English et al. [2]:

$$w_g' = 0.286 \frac{d_h^{0.322} \rho_l^{0.419} \sigma^{0.097}}{\rho_g^{0.462} \eta_l^{0.15} w_l'^{0.075}}. \tag{4}$$

When the calculation is carried out in SI units, this equation yields the superficial flooding velocity in m/s.

In the ESDU data item on reflux condensation [3], data of the heat transfer coefficient of reflux condensation experiments in vertical tubes have been compared with results of correlations for gravity controlled cocurrent flow of vapour and condensate. Due to the proximity of the experimental reflux condensation data to the respective correlations for cocurrent flow, it is recommended in the ESDU data item to use these correlations also in the reflux situation. The correlations for different ranges of the condensate film Reynolds number are, respectively, those of Nusselt [4] ($Re \leqslant 7.5$, Eq. (6)), Kutateladze [5] ($7.5 < Re < 400$, Eq. (7)) and Labuntsov ($Re \geqslant 400$, see [6]).

The condensate film Reynolds number is defined as follows:

$$Re = \frac{\dot{M}}{\pi d \eta_l}. \tag{5}$$

The recommended correlations for the condensate film Reynolds number ranges $Re \leqslant 7.5$ and $7.5 < Re < 400$ are as follows:

$$Re \leqslant 7.5 : Nu_m = 0.925 Re^{-1/3}, \tag{6}$$

$$7.5 < Re < 400 : Nu_m = \frac{Re}{1.47 Re^{1.22} - 1.3}. \tag{7}$$

The mean Nusselt number is defined as

$$Nu_m = \frac{\alpha_m (v_l^2/g)^{1/3}}{\lambda_l}. \tag{8}$$

Wang and Ma [7] carried out theoretical and experimental studies on vertical and inclined thermosyphons. They pointed out that no final conclusion can be drawn on the optimum inclination angle at which the maximum heat transfer coefficient occurs because it is not independent from operating conditions. Wang and Ma presented the following semi-empirical correlation for reflux condensation heat transfer:

$$\frac{Nu_{\mathrm{m}}}{Nu_{\mathrm{m},n}} = \left(\frac{L}{R}\right)^{\cos\beta/4} (0.54 + 5.68 \times 10^{-3}\beta). \quad (9)$$

$Nu_{\mathrm{m},n}$ is the average Nusselt number according to the classical Nusselt film theory [4] for condensation in a vertical tube (Eq. (6)). For condensation in a vertical tube (inclination angle $\beta = 90°$) this semi-empirical correlation predicts:

$$Nu_{\mathrm{m}} = 1.07 Nu_{\mathrm{m},n}. \quad (10)$$

Hassan and Jakob [8] analysed laminar film condensation of pure saturated vapours on the outside of inclined circular cylinders. Their analysis is made under the same assumptions as Nusselt's classical theory of film condensation [4]. Hassan and Jakob compared their analytical results with experimental results for the heat transfer coefficient during cocurrent condensation of steam inside an inclined tube (∅ 31.8 mm). The experimental results were found to be 28–100% higher than the analytical results. Hassan and Jakob ascribed this deviation to the rippling of the condensate film that is not taken into account in the model.

Fürst [9] as well as Fieg and Roetzel [10] developed models for the calculation of condensation in an inclined elliptical tube. In the model of Fieg it is assumed that the condensate drains as a laminar film at the circumference of the tube and accumulates in the lowermost part of the tube in a condensate layer that drains likewise in a laminar manner. The different regions arising out of this assumption are calculated separately but are linked by boundary conditions. Fieg [11] presented an analytical solution for the local film thickness on the outside of an inclined elliptical tube for Nusselt-type condensation. Surface tension effects are taken into account.

2. Experimental setup and method

Experiments were carried out with refrigerant R134a, as it represents fluid properties that are similar to those of process fluids, e.g. the density ratio of vapour and liquid. Due to the relatively low surface tension of R134a a continuous condensate film is formed, i.e. film condensation occurs. Fig. 1 shows the experimental setup. The forced flow in-tube evaporator W1 provides saturated or superheated vapour. It is a coaxial coiled evaporator. The entering liquid is completely evaporated when passing through the evaporator. The mass flow rate of vapour that exits the evaporator is therefore equal to the liquid that enters the evaporator. The mass flow rate of the liquid is determined by a coriolis mass flow meter (accuracy ± 0.15%) before entering the evaporator. The vapour enters the test section slightly superheated at the bottom. At the vapour outlet of the test section a sight glass is located to be able to determine visually the flooding point. Also the ultrasonic pulse-echo technique can be used to identify the flooding point (see below). The part of the vapour that is not condensed in the test section is liquefied in the secondary condenser W2. The condensate is returned to the flow return circuit which consists of the header tank B1, the pump P1 and a filter/dryer for the refrigerant.

The condensate that exits the test section at the bottom passes through the volumetric cylinder B2. The flow rate of condensate was determined by collecting condensate in this cylinder for a known period of time. From the volumetric cylinder the condensate is as well returned to the flow return circuit. From there the liquid is pumped again to the evaporator.

The test section is a 500 mm long double pipe heat exchanger made of stainless steel. Condensation takes place in the inner tube. Fig. 2 shows the inlet header of the test section. The inner diameter of the inner tube is 7 mm. The pressure drop between inlet and outlet of the test section was measured by a differential pressure transducer (accuracy ± 0.5%). Temperature controlled cooling water flows in the annulus of the test section counter-currently to the vapour in the inner tube. The cooling water flow rate is determined with an impeller flow meter (accuracy ± 2.5%). To be able to vary the inclination angle the test section is connected by flexible pressure hoses.

Twenty K-type thermocouples (∅ 0.25 mm) are embedded 0.2 mm beneath the inner tube surface in the inner tube wall around the circumference of the test section to be able to measure local wall temperatures. The tube wall thickness is 0.5 mm. The thermocouple leads are silver-soldered into axial grooves (10 mm long, 0.3 mm wide, 0.3 mm deep) and taken out through the annulus and fittings in the outer tube wall located 15 mm downstream in flow direction of the coolant. The thermocouples are located at five different axial positions of the test section, at each axial position four thermocouples are embedded around the circumference of the tube: one at the top, one at the bottom and one at each side (for further details refer to [14]).

The reflux condensation heat transfer experiments were carried out at system pressures between 0.67 and 0.74 MPa at the inlet of the test section and at inclination angles of 30°, 45°, 60° and 90° from the horizontal. The vapour entered the test section about 1 K

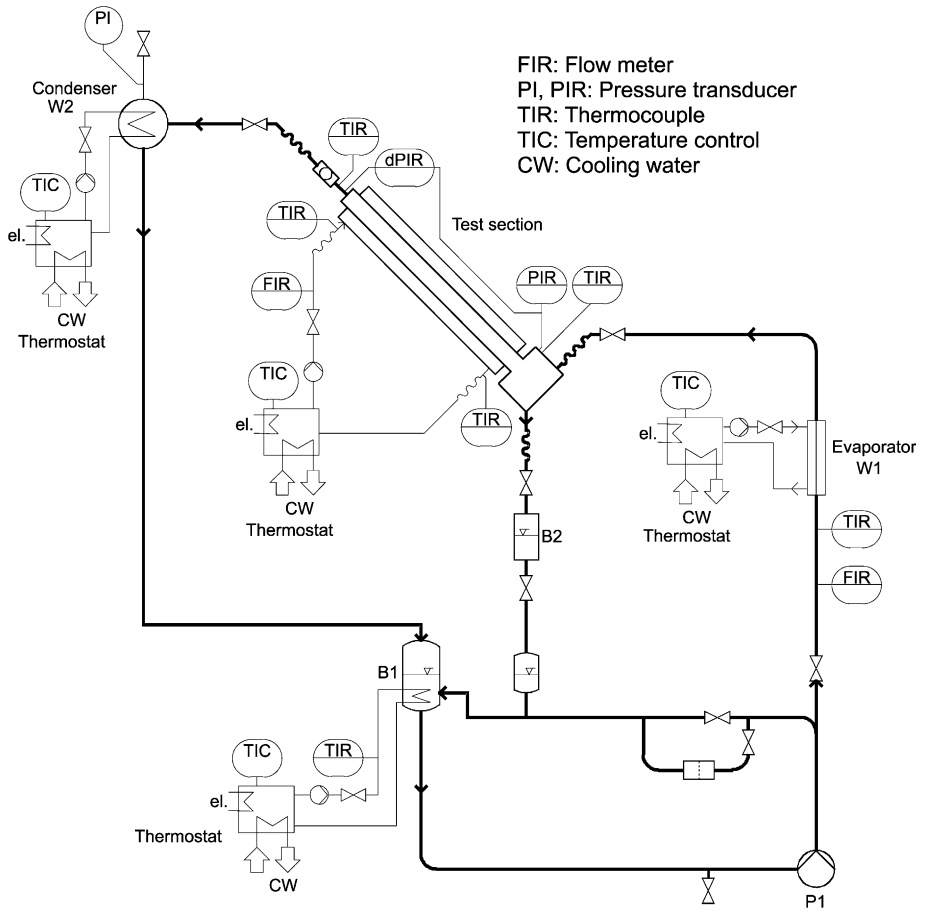

Fig. 1. Schematic of experimental setup.

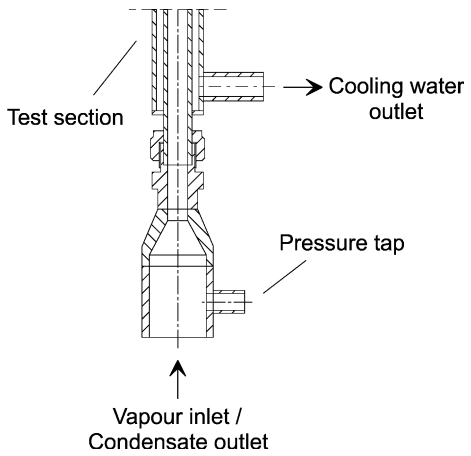

Fig. 2. Inlet header of test section.

superheated. The mean condensation heat transfer coefficient was calculated from

$$\alpha_m = \frac{\dot{Q}}{\pi d L (T_S - T_W)}. \tag{11}$$

T_S is the saturation temperature of the vapour. The wall temperature T_W is the arithmetic mean value of the local inner wall temperatures. The arithmetic mean value of the measured local inner wall temperatures can be taken directly as the inner wall surface temperature, as the temperature difference between the location of the thermocouples and the inner wall surface is only 0.1 K or less for the heat fluxes at which the experiments were performed. This uncertainty was assumed to be tolerable.

The total heat transfer $\dot{Q}$ was determined from the flow rate of the cooling water and the temperature rise as well as computed from the measured condensate flow rate:

$$\dot{Q} = \dot{M}_{CW} c_{p,CW} \Delta T, \tag{12}$$

$$\dot{Q} = \dot{M}_{cond} \Delta h_v. \tag{13}$$

The difference between the two heat flow rates was usually smaller than ±10%. A test run was repeated if the deviation was larger than ±12%. Once the mean condensation heat transfer coefficient was established the mean Nusselt number could be obtained according to Eq. (8). The condensate film Reynolds number was calculated from Eq. (5).

Flooding was established by increasing the vapour flow rate while keeping the cooling water flow rate and the inlet cooling water temperature constant. Flooding could be observed visually through a sight glass located at the top outlet of the test section: Condensate then left the test section at the top. Also the ultrasonic pulse-echo technique can be used to determine the flooding point (see below). Measurements were carried out slightly before the flooding point was reached so that all condensate could be collected at the bottom of the tube.

The superficial vapour velocity is calculated from the measured vapour mass flow rate:

$$w'_{\mathrm{g}} = \frac{\dot{M}_{\mathrm{g}}}{\rho_{\mathrm{g}} A}. \tag{14}$$

From the total heat transfer $\dot{Q}$ (see Eqs. (12) and (13)) the superficial condensate velocity is determined:

$$w'_{\mathrm{l}} = \frac{\dot{Q}}{\Delta h_{\mathrm{v}} \rho_{\mathrm{l}} A}. \tag{15}$$

A conventional ultrasonic transducer was used to measure the condensate film thickness before the onset of flooding. A schematic is shown in Fig. 3a. The piezoelectric transducer (3 mm diameter) and its acrylic supporter is attached to the outside of the tube wall. It emits a 15 MHz ultrasonic signal which is reflected at each interface. The transducer also works as a receiver and detects the reflected signals.

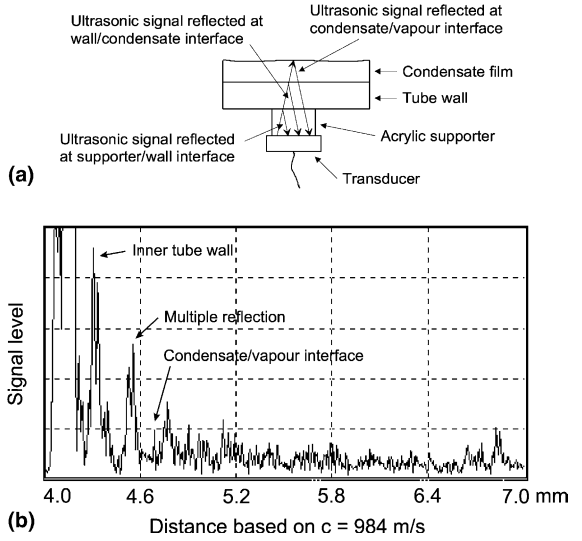

Fig. 3. Pulse-echo technique: (a) schematic of ultrasonic transducer attached to the tube wall and (b) signal with condensate film of R134a.

When the time lag Δt between the reflections of the signal from the wall/condensate interface and from the condensate/vapour interface is determined and the sound speed c in the liquid is known the film thickness δ can be calculated:

$$\delta = \frac{c \cdot \Delta t}{2}. \tag{16}$$

Fig. 3b shows a typical output signal for the transducer being attached to the inner tube of the test section with a condensate film of R134a inside. Each distinct peak occurs due to a reflection at an interface. There are also peaks due to multiple reflections. The exact distance between the peaks can be determined by means of a software that is part of the used commercially available ultrasonic system.

When the flooding point is reached condensate bridges occur that close the entire cross-section of the tube for short moments. Therefore at the flooding point there is no echo of the phase interface condensate/vapour but an additional echo of the opposite tube wall. The distance between the echo of the inner tube wall and the flooding echo corresponds to the inner tube diameter.

The pulse-echo technique is non-intrusive, a calibration is not necessary if the sound velocity in the liquid is known, and even very small film thicknesses can be detected. An advantage of this technique is the possibility of determining liquid film thicknesses in non-transparent pipes, i.e. also in metallic pipes. However, so far the use of the pulse-echo technique in two-phase flow applications is rather limited (see [12]).

3. Modelling

The model for reflux condensation of a pure saturated vapour in an inclined tube that is described below is based on models proposed by Hassan and Jakob [8] as well as by Fürst [9]. Fig. 4 shows a differential control volume of the condensate film inside the tube that is inclined at an angle β to the horizontal. The control volume is acted upon by the force of gravity in circumferential and in axial direction. Therefore condensate flows in circumferential as well as in axial direction. The saturated vapour enters the tube at the bottom and flows upwards, i.e. in negative z-direction. The surface temperature of the inner tube wall is T_{W}. The condensate film at the phase interface is at the saturation temperature T_{S}. The condensate drains as a smooth laminar film tangential to the tube wall in x- and z-direction. The condensate accumulates in the lowermost part of the

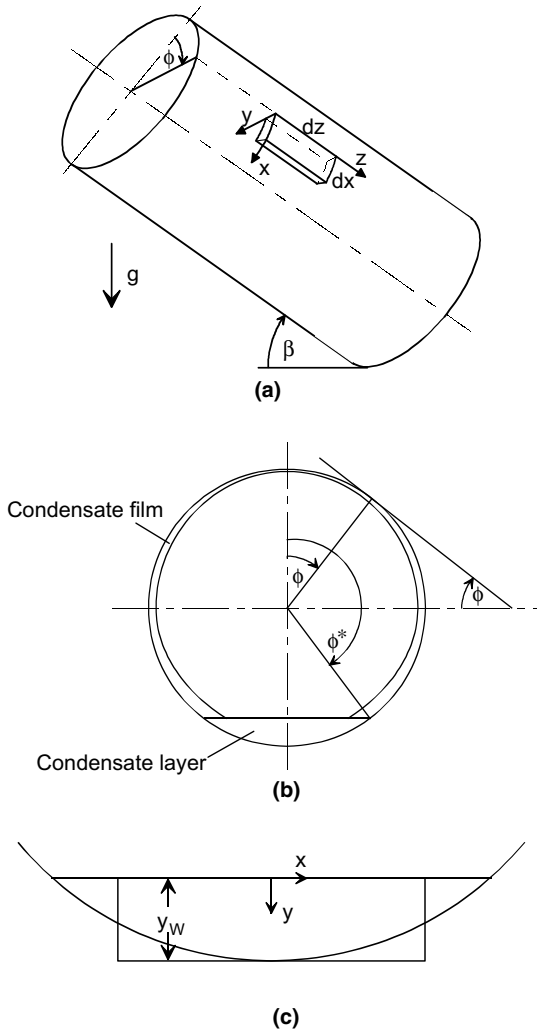

Fig. 4. Modelling: (a) differential control volume of the condensate film inside the tube, (b) distribution of condensate inside the tube and (c) condensate layer at lowermost point of tube.

tube and drains gravity-controlled in a condensate layer in z-direction. The height of this condensate layer is given by the angle ϕ^* (see Fig. 4b). Consequently there are two distinct regions: The condensate film that drains at the circumference of the tube and the condensate layer in the lowermost part of the tube. In the following the modelling of these two regions is described separately.

3.1. Condensate film flow at the circumference of the tube

The following simplifying assumptions are made:

- The vapour is pure and saturated.
- The condensate film is smooth and laminar.
- The shear stress on the condensate film caused by the vapour is negligible (this assumption was confirmed in own experiments (see [13])).
- The pressure drop of the vapour is negligible (confirmed in own experiments (see [13])). Hence the temperature at the interface is uniform and equal to the saturation temperature.
- The temperature at the inner tube wall is uniform and constant.
- The velocity distribution at any point in the condensate film is the same as that in a fully developed film flowing on a plane tangential to the surface at that point. Consequently the curvature of the tube wall is neglected.
- The film thickness is small compared to the tube diameter.
- The latent heat liberated by the condensing vapour is transferred by heat conduction across the condensate film. The convective heat transfer is neglected.
- The physical properties of the condensate are constant.

Assuming a steady-state flow, the forces exerted by the shear stresses are in equilibrium with gravity. The following differential equations for the velocity components in x- and z-direction are obtained from a balance of forces acting on a differential control volume of the condensate film (Fig. 4a) according to the classical Nusselt film condensation theory:

$$\eta_l \frac{\partial^2 w_x}{\partial y^2} + (\rho_l - \rho_g) g \sin\phi \cos\beta = 0, \tag{17}$$

$$\eta_l \frac{\partial^2 w_z}{\partial y^2} + (\rho_l - \rho_g) g \sin\beta = 0. \tag{18}$$

The boundary conditions are as follows:

$$y = 0: \quad w_x = w_z = 0 \tag{19}$$

$$y = \delta: \quad \frac{\partial w_x}{\partial y} = \frac{\partial w_z}{\partial y} = 0 \tag{20}$$

An integration yields the velocity components in x- and z-direction:

$$w_x = \frac{(\rho_l - \rho_g) g \sin\phi \cos\beta}{\eta_l} \left(\delta y - \frac{y^2}{2} \right), \tag{21}$$

$$w_z = \frac{(\rho_l - \rho_g) g \sin\beta}{\eta_l} \left(\delta y - \frac{y^2}{2} \right). \tag{22}$$

The mean velocities are obtained by an integration across the film thickness:

$$w_{m,x} = \frac{1}{\delta} \int_0^\delta w_x \, dy = \frac{(\rho_l - \rho_g) g \sin\phi \cos\beta}{3\eta_l} \delta^2, \tag{23}$$

$$w_{\mathrm{m},z} = \frac{1}{\delta}\int_0^{\delta} w_z \,\mathrm{d}y = \frac{(\rho_\mathrm{l}-\rho_\mathrm{g})g\sin\beta}{3\eta_\mathrm{l}}\delta^2. \tag{24}$$

The mass flow rate in x- and z-direction can be expressed as follows:

$$\dot{M}_x = w_{\mathrm{m},x}\rho_\mathrm{l}\delta\,\mathrm{d}z, \tag{25}$$

$$\dot{M}_z = w_{\mathrm{m},z}\rho_\mathrm{l}\delta\,\mathrm{d}x. \tag{26}$$

By formation of the condensate mass flow rate $\mathrm{d}\dot{M}$ the heat flow rate

$$\mathrm{d}\dot{Q} = \Delta h_\mathrm{v}\,\mathrm{d}\dot{M} \tag{27}$$

is liberated. According to the assumptions made above this heat flow rate is transferred by pure heat conduction across the condensate film. Thus the heat flow rate transferred in a surface element $\mathrm{d}x\,\mathrm{d}z$ is

$$\mathrm{d}\dot{Q} = \frac{\lambda_\mathrm{l}}{\delta}\Delta T\,\mathrm{d}x\,\mathrm{d}z. \tag{28}$$

From Eqs. (27) and (28) follows:

$$\Delta h_\mathrm{v}\mathrm{d}\dot{M} = \frac{\lambda_\mathrm{l}}{\delta}\Delta T\,\mathrm{d}x\,\mathrm{d}z. \tag{29}$$

The vapour condensing on a surface element causes an increase of the condensate mass flow rate in circumferential direction (x-direction) as well as in axial direction (z-direction).

Therefore Eq. (29) can be written as

$$\Delta h_\mathrm{v}\left(\frac{\partial\dot{M}_x}{\partial x}\mathrm{d}x + \frac{\partial\dot{M}_z}{\partial z}\mathrm{d}z\right) = \frac{\lambda_\mathrm{l}}{\delta}\Delta T\,\mathrm{d}x\,\mathrm{d}z. \tag{30}$$

By combining Eqs. (23)–(26) with Eq. (30) the following partial differential equation for the local film thickness $\delta(\phi, z)$ is obtained (with $\mathrm{d}x = R\,\mathrm{d}\phi$):

$$\delta^4\cos\phi\cos\beta + 3\delta^3\cos\beta\sin\phi\frac{\partial\delta}{\partial\phi} + 3\delta^3 R\sin\beta\frac{\partial\delta}{\partial z} = \frac{3\lambda_\mathrm{l}\Delta T\eta_\mathrm{l}R}{\rho_\mathrm{l}(\rho_\mathrm{l}-\rho_\mathrm{g})g\Delta h_\mathrm{v}}. \tag{31}$$

Eq. (31) is also applicable to the cases "vertical tube" and "horizontal tube": substituting $\beta = \pi/2$ in Eq. (31) reduces it to that for condensation on a vertical plate that is in case of $\delta \ll d$ also valid for vertical tubes (Nusselt [4]). By substituting $\beta = 0$ in Eq. (31) the partial differential equation for condensation at the outside of a horizontal tube is obtained (Nusselt [4]).

With the abbreviations

$$\Psi = \frac{\rho_\mathrm{l}(\rho_\mathrm{l}-\rho_\mathrm{g})g\Delta h_\mathrm{v}\cos\beta}{3\lambda_\mathrm{l}\Delta T\eta_\mathrm{l}R}\delta^4 \tag{32}$$

and

$$Z = \frac{z}{R\tan\beta} \tag{33}$$

Eq. (31) becomes

$$\frac{\partial\psi}{\partial Z} + \sin\phi\frac{\partial\psi}{\partial\phi} = \frac{4}{3}(1-\Psi\cos\phi). \tag{34}$$

Two boundary conditions are required to obtain the solution of Eq. (34). At the top of the tube the film thickness equals zero:

$$Z = 0: \quad \Psi = 0. \tag{35}$$

Due to symmetry of the condensate film the gradient of condensate film thickness at the uppermost point of the tube is zero along the entire length of the tube:

$$\phi = 0: \quad \frac{\partial\Psi}{\partial\phi} = 0 \tag{36}$$

Eq. (34) was solved numerically using finite differences (refer to [14]).

3.2. Condensate layer in the lowermost part of the tube

The condensate formed at the circumference of the tube accumulates in the lowermost part of the tube and drains gravity-controlled in z-direction. The following simplifying assumptions are made:

- The condensate layer is smooth and laminar.
- The shear stress on the condensate film caused by the vapour is negligible.
- The pressure drop of the vapour is negligible.
- Since the condensate layer is considerably thicker than the condensate film at the circumference of the tube the heat transferred through the condensate layer is neglected.
- The condensate layer is in stationary, developed flow.

Under these assumptions the simplified Navier–Stokes equation for the condensate layer is:

$$\eta_\mathrm{l}\left(\frac{\partial^2 w_\mathrm{CL}}{\partial x^2} + \frac{\partial^2 w_\mathrm{CL}}{\partial y^2}\right) + (\rho_\mathrm{l}-\rho_\mathrm{g})g\sin\beta = 0. \tag{37}$$

Differing from the model for the condensate film flow at the circumference of the tube the origin of the coordinate system is now at the surface of the condensate layer (see Fig. 4c).

Assuming that the width of the condensate layer in the lowermost part of the tube is much bigger than its height the following relation applies:

$$\frac{\partial^2 w_\mathrm{CL}}{\partial x^2} \ll \frac{\partial^2 w_\mathrm{CL}}{\partial y^2}. \tag{38}$$

The velocity distribution in the condensate layer is calculated under the assumption that the condensate drains in a rectangular cross-section (see Fig. 4c). This simplification was also made by Fürst [9] as well as by

others (e.g. Moalem Maron and Sideman [15]). Taking Eq. (38) into account Eq. (37) can be simplified:

$$\frac{\partial^2 w_{CL}}{\partial y^2} = -\frac{(\rho_l - \rho_g) g \sin\beta}{\eta_l}. \tag{39}$$

The following boundary conditions apply:

$$y = 0: \quad \frac{\partial w_{CL}}{\partial y} = 0. \tag{40}$$

$$y = y_W: \quad w_{CL} = 0. \tag{41}$$

The solution of Eq. (39) is:

$$w_{CL} = \frac{(\rho_l - \rho_g) g \sin\beta}{2\eta_l}(y_W^2 - y^2). \tag{42}$$

The mean velocity is obtained by integration across the height of the condensate layer:

$$w_{m,CL} = \frac{1}{\delta}\int_0^\delta w_{CL}\,dy = \frac{(\rho_l - \rho_g) g \sin\beta}{3\eta_l} y_W^2. \tag{43}$$

The mass flow rate of the condensate layer is

$$\dot{M}_{CL} = w_{m,CL}\rho_l A_{CL}. \tag{44}$$

The cross-sectional area A_{CL} of the condensate layer is related to the angle ϕ^* and the radius R:

$$A_{CL} = \frac{R^2}{2}(2\cdot(180^\circ - \phi^*) - \sin(2\cdot(180^\circ - \phi^*))). \tag{45}$$

The mass flow rate of the condensate layer increases in axial direction due to condensation at the circumference of the tube. The increase per unit tube length follows from the flow rate of the draining condensate from the sides of the tube and can be calculated as (see [14])

$$\frac{d\dot{M}_{CL}}{dz} = \frac{2\rho_l(\rho_l - \rho_g) g \sin\phi^* \cos\beta \delta^3}{3\eta_l}. \tag{46}$$

Based on the calculated film thickness at the circumference of the tube (solution of Eq. (31)) and under consideration of Eqs. (44) and (45) the angle ϕ^* can be iteratively determined.

3.3. Heat transfer coefficient

From the values of ψ (solution of Eq. (34)) local values of the heat transfer coefficient can be obtained. Under the assumptions made the local heat transfer coefficient is

$$\alpha = \frac{\lambda_l}{\delta}. \tag{47}$$

By rearranging Eq. (32) to δ and inserting it into Eq. (47) one obtains:

$$\alpha = \left(\frac{\rho_l(\rho_l - \rho_g) g \Delta h_v \lambda_l^3 \cos\beta}{3\eta_l \Delta T R}\frac{1}{\Psi}\right)^{1/4}. \tag{48}$$

From the local heat transfer coefficients a mean heat transfer coefficient can be calculated at each distance Z for an infinitesimal ring on the tube surface:

$$\alpha_M = \frac{1}{\pi}\int_0^{\phi^*} \alpha\,d\phi. \tag{49}$$

The local heat transfer coefficients are integrated only up to the angle ϕ^* because the heat transferred through the condensate layer is assumed to be negligible.

The mean heat transfer coefficient for the entire surface of the inclined tube can be obtained from

$$\alpha_m = \frac{1}{L}\int_0^L \alpha_M\,dz. \tag{50}$$

4. Results and discussion

4.1. Flooding data

In Fig. 5a the experimental flooding data are presented in terms of the square root of the dimensionless superficial velocities. The given inclination angles are the angles from the horizontal. It can be seen that the inclination angle as well as the system pressure have a significant effect on the flooding point for reflux condensation of R134a. At a higher pressure the momentum flux required to initiate flooding can be reached at a lower absolute superficial flooding vapour velocity due to a higher ratio of vapour to liquid density. Consequently the absolute superficial flooding vapour velocity decreases with an increasing system pressure. However, due to the definitions of the dimensionless velocities the dimensionless superficial flooding vapour velocity increases with an increasing system pressure for all inclination angles, as can be seen in Fig. 5a. The optimum inclination angle at which the highest flooding vapour velocity occurs is between 45° and 60° from the horizontal. This trend is also shown in Fig. 5b for two different superficial liquid velocities. When the tube is tilted from the vertical the condensate at the bottom end of the tube does not drain around the entire circumference but only in the lowermost part. The opposite flowing vapour can enter the tube in the upper region of the cross-section. Therefore the flooding point is reached only at higher vapour velocities. The further the tube is tilted from the vertical, the smaller becomes the fraction of gravity that causes the drainage of the condensate in axial direction. Consequently in tubes that are only slightly inclined to the horizontal flooding occurs again at lower vapour velocities.

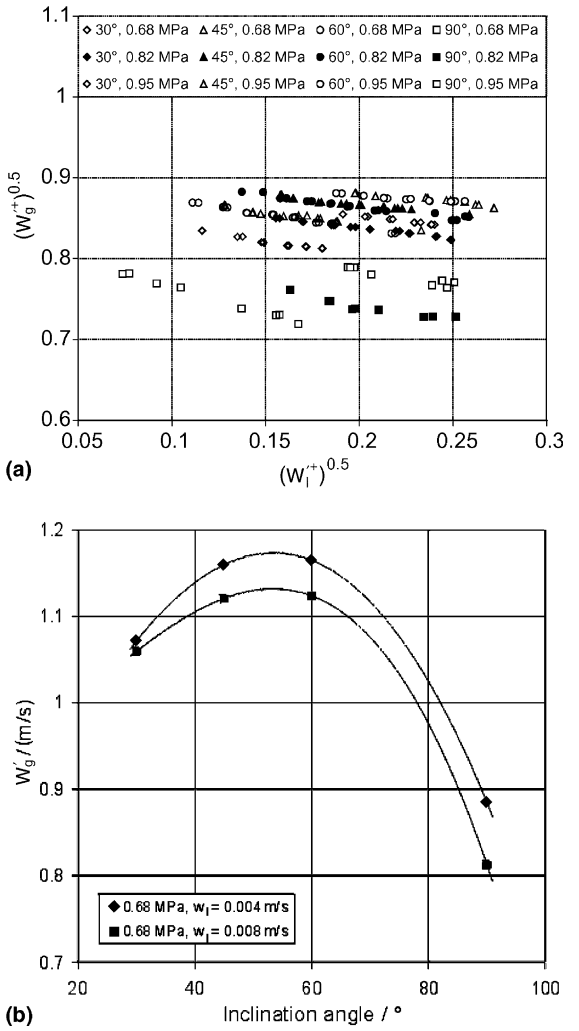

Fig. 5. Experimental flooding data for reflux condensation of R134a: (a) square root of the dimensionless superficial vapour velocity vs. liquid velocity and (b) effect of inclination angle on flooding vapour velocity.

The experimental flooding data were compared with various flooding correlations that can be found in the literature (e.g. Mouza et al. [1], McQuillan and Whalley [16], Zapke and Kröger [17,18] (refer to Fiedler et al. [19])). The correlation by English et al. [2] (Eq. (4)) showed the best agreement with the own experimental data obtained with R134a. However, this correlation does not take into account the effect of the inclination angle β on flooding. Therefore a term was added to consider inclination that is similar to an added term proposed by Chen [20]:

$$w'_g = 0.45(\sin 1.7\beta)^{0.38} \frac{d^{0.322}\rho_l^{0.419}\sigma^{0.097}}{\rho_g^{0.462}\eta_l^{0.15}w_l'^{0.075}}. \quad (51)$$

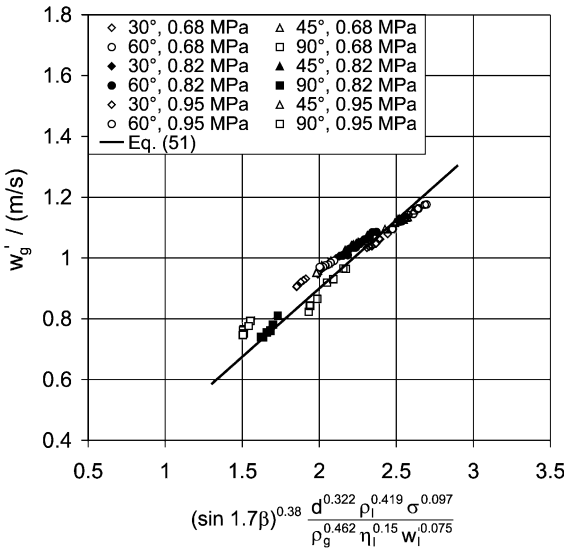

Fig. 6. Comparison of experimental flooding data for R134a with proposed modified English-correlation.

As can be seen in Fig. 6 the modified English correlation agrees well with the own experimental data for R134a for all inclination angles. However, comparisons with other fluids and other geometries have shown that—among other things—surface tension has a major effect (refer to [21,22]). Therefore Eq. (51) is only valid for reflux condensation of R134a in the examined tube geometry. Fluids possessing a significantly different surface tension or density ratio between vapour and condensate may not be covered by Eq. (51).

4.2. Heat transfer

The experimental reflux condensation heat transfer data are depicted in Fig. 7a. They are presented—as usual in gravity controlled condensation—in terms of the mean condensate film Nusselt number and the condensate film Reynolds number at the bottom end of the tube. It can be seen that the inclination angle has a strong effect on the condensation heat transfer. The average Nusselt number is smallest for reflux condensation in the vertical position ($\beta = 90°$). The Nusselt number increases when the tube is tilted from the vertical because then the film thickness is no longer axisymmetric. Due to gravity the condensate film becomes very small in the upper region of the tube while a thicker stream of condensate drains in the lowermost part of the tube. The mean film thickness decreases and therefore the mean heat transfer coefficient increases. Fig. 7b shows the effect of the inclination angle on the condensation heat transfer for constant film Reynolds numbers of $Re \approx 75$ and $Re \approx 100$. In this diagram also trendlines are depicted. It can be seen that according to the

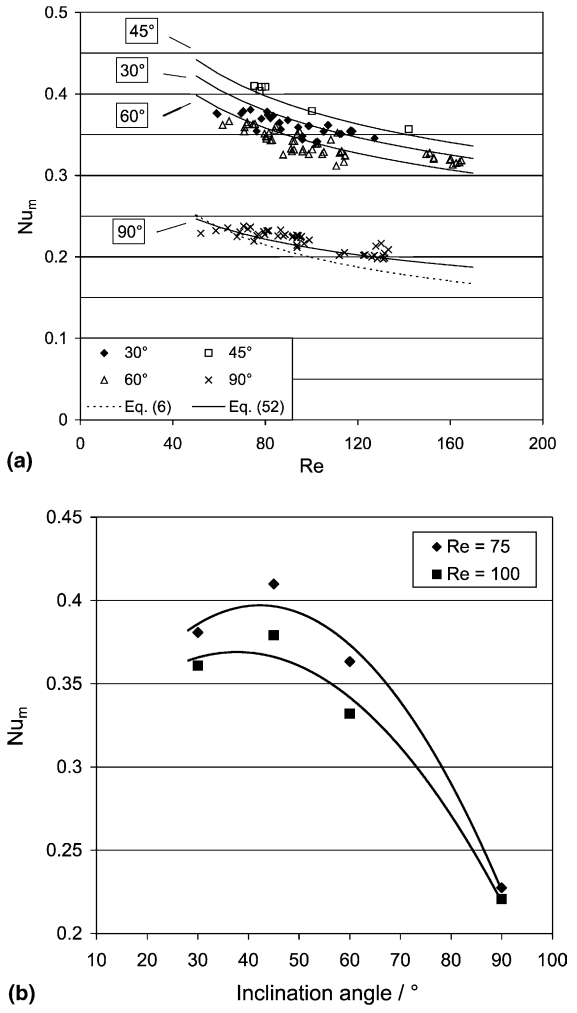

Fig. 7. Experimental heat transfer data for reflux condensation of R134a: (a) mean condensate film Nusselt number vs. condensate film Reynolds number at bottom end of tube and (b) effect of inclination angle on reflux condensation heat transfer.

experimental data the optimum inclination angle for the heat transfer lies close to 40° from the horizontal.

The experimental reflux condensation heat transfer data were compared with values predicted by the classical Nusselt theory for condensation in a vertical tube [4] (Eq. (6)). As can be seen in Fig. 7a the classical Nusselt correlation only very slightly underpredicts the experimental data for the vertical tube. A modified semi-empirical correlation, originally suggested by Wang and Ma [7], was proposed to predict the average Nusselt number in dependence of the condensate film Reynolds number and the inclination angle:

$$\frac{Nu_{\mathrm{m}}}{Nu_{\mathrm{m},k}} = \left(\frac{L}{R}\right)^{\cos\beta/4} (0.125 + 1.46\times10^{-2}\beta - 7.27\times10^{-5}\beta^2) \quad (52)$$

In this correlation the average Nusselt number is related to the one predicted by Kutateladze [5] (Eq. (7)) for condensation in a vertical tube. As can be seen in Fig. 7a the modified Wang/Ma correlation agrees well with the experimental data for all inclination angles.

4.3. Analytic results

From the values of ψ (see Eq. (34)) local values of the thickness of the condensate film at the circumference of the tube can be obtained. Fig. 8a shows the dimensionless film thickness vs. the dimensionless distance (see Eq. (33)) and the peripheral angle ϕ according to the model for the condensate film flow at the circumference of the tube (solution of Eq. (31)). In the inclined tube the condensate film thickness approaches a limiting value at any angular position except at $\phi = 180°$. The reason for this finite film thickness in the major part of the surface of the tube wall is that the liquid is always moved to a lower point on the surface by the gravitational force. It is remarkable that the limiting value of the condensate film thickness is reached within a relative short dimensionless distance.

The model for the condensate film flow at the circumference of the tube does not well characterise the actual conditions in the lowermost part of the tube due to the neglect of the curvature of the tube wall. According to the model for the condensate flow at the circumference of the tube the entire condensate accumulates only at the point $\phi = 180°$. But in fact the amount of condensate is distributed over a wider range (see Fig. 4b). Therefore the condensate layer in the lowermost part of the tube is calculated according to the model outlined in Section 3.2. Fig. 8b exemplifies the calculated height y_{W} of the condensate layer at the lowermost point of the tube for condensation of R134a at a pressure of 0.72 MPa and a wall subcooling of 6.5 K in a tube with an inner diameter of 7 mm and a length of 500 mm.

As expected the film thickness increases for all inclination angles with increasing axial position due to condensation. The film thickness in the vertical tube is considerably smaller than the height of the condensate layer at the lowermost point of the inclined tubes because in the vertical tube the condensate is distributed uniformly around the whole circumference. Due to the same reason the curves for the inclined tubes are at a steeper slope than the curve for the vertical tube.

Fig. 8c shows the mean heat transfer coefficient α_{M} for an infinitesimal ring on the tube surface vs. the length of the tube. The calculation was again carried out for condensation of R134a at a pressure of 0.72 MPa and a wall subcooling of 6.5 K in a tube with an inner diameter of 7 mm and a length of 500 mm.

For the inclined tubes the mean heat transfer coefficient for an infinitesimal ring on the tube surface initially

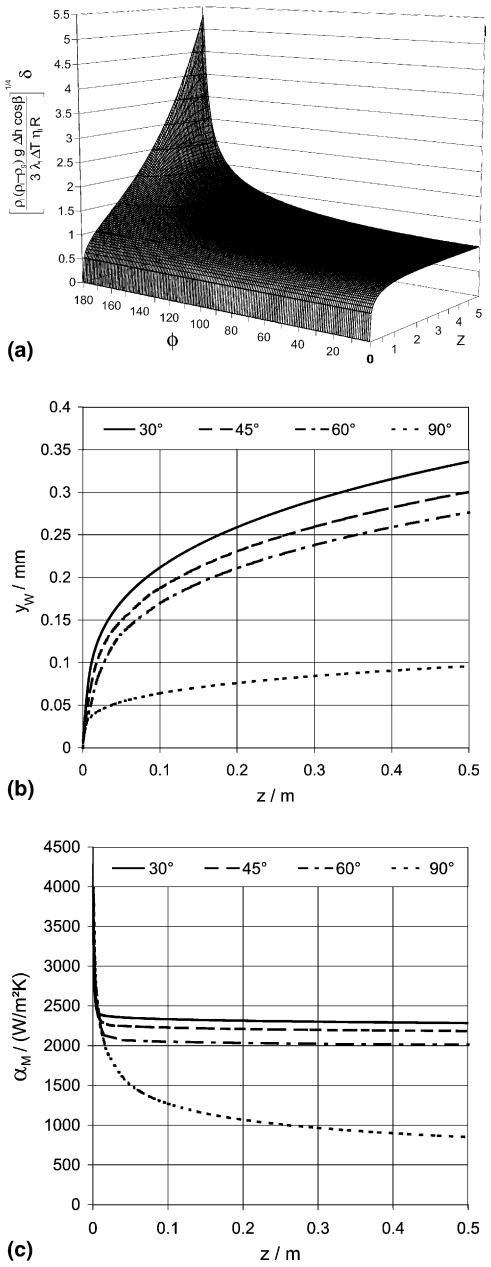

Fig. 8. Analytic results: (a) dimensionless film thickness vs. dimensionless distance Z and peripheral angle ϕ, (b) height of condensate layer at lowermost point of tube (condensation of R134a, $p = 0.72$ MPa, $\Delta T = 6.5$ K) and (c) mean heat transfer coefficient α_M vs. the length of the tube (condensation of R134a, $p = 0.72$ MPa, $\Delta T = 6.5$ K).

decreases sharply but approaches after a rather short axial distance a value that decreases only slightly. This behaviour is due to the fact that—as already mentioned above—the film thickness in the upper part of the tube reaches a limiting value that does not change in axial direction. At an inclination angle of 30° this limiting value is established after the shortest distance in axial direction because of the shortest peripheral distance in direction of the gravitational force. The further slight decrease of the heat transfer coefficient at distances at which the limiting value of the film thickness is already reached is caused by the increase in height of the condensate layer at the lowermost point of the tube. At the smallest inclination angle the highest heat transfer coefficient is reached because at this inclination angle the peripheral distance in direction of the gravitational force is the shortest and therefore the film thickness is the smallest. But on the other hand at the smallest inclination angle the fraction of the gravitational force in axial direction, that causes the drainage of the condensate layer at the lowermost point of the tube, is smallest. This effect in turn deteriorates the heat transfer coefficient at small inclination angles. For the vertical tube the heat transfer coefficient decreases steadily as the film thickness increases steadily around the whole circumference of the tube.

Table 1
Mean heat transfer coefficients α_m for the entire surface of the tube

Inclination angle	30°	45°	60°	90°
α_m/(W/m^2 K)	2320	2220	2049	1139

The mean heat transfer coefficients α_m for the entire surface of the tube that were calculated according to Eq. (50) for the curves shown in Fig. 8c are given in Table 1. For this example the mean heat transfer coefficient is at an inclination angle between 30° and 45° about twice as high as for the vertical tube. This means that the condensation heat transfer can be considerably improved by inclining the tube. This effect has been confirmed by the experimental data (see Fig. 7b).

4.4. Comparison of calculated values with experimental data

The results for the mean heat transfer coefficient and the film thickness at the lowermost point of the tube are compared with own experimental data for reflux condensation of refrigerant R134a. The heat transfer data were presented in Section 4.2. The film thickness measurements have been carried out with the ultrasonic pulse-echo technique. Experiments were conducted at inclination angles of 30°, 45°, 60° and 90° from the horizontal.

The calculations are carried out with the physical properties of R134a and the temperature differences that occurred in the experiments. The temperature difference between the vapour and the tube wall is taken as the difference between the saturation temperature of the

vapour and the arithmetic mean value of the measured local wall temperatures. Fig. 9a shows a comparison between the experimental heat transfer coefficients and the calculated values. In spite of the simplified model the theoretical values are in good agreement with the experimental data. The calculated heat transfer coefficients for the inclined tube are somewhat larger than the experimental data.

A possible reason for this deviation could be that the draining condensate is slightly retarded by the countercurrently flowing vapour. This would increase the film thickness and deteriorate the heat transfer. In the model the influence of the vapour flow is neglected. However, in our own experiments with R134a it was found that the vapour velocity has no significant effect on the heat transfer for vapour velocities well below the flooding point. Nevertheless this effect depends on fluid properties such as, for example, the density ratio between vapour and condensate.

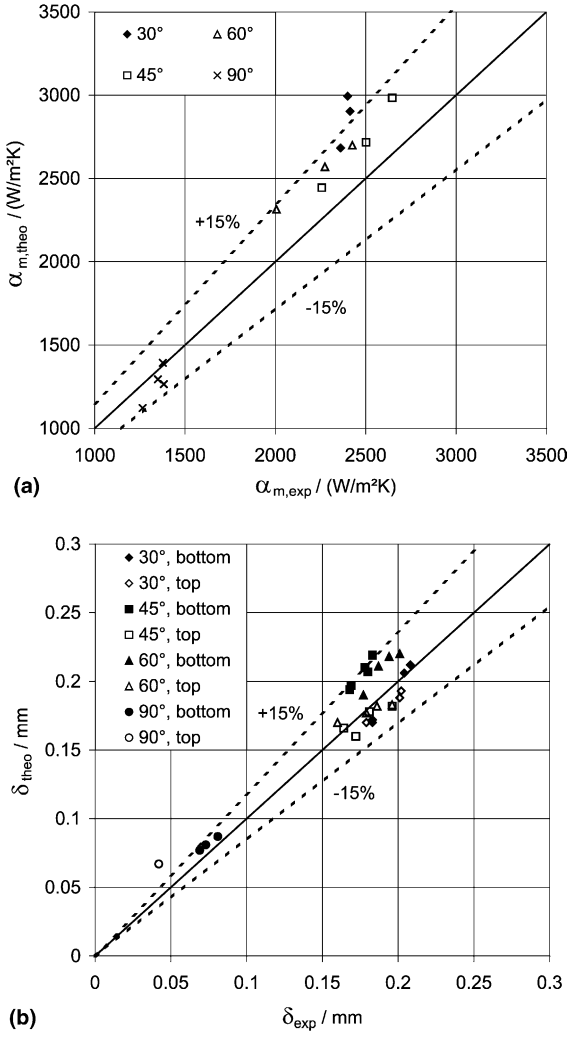

Fig. 9. Comparison of theoretical and experimental values: (a) mean heat transfer coefficient and (b) condensate film thickness ("top": at a position $z = 171$ mm, "bottom": at a position $z = 476$ mm).

Another possible reason for the deviation is that due to the surface tension the condensate film thickness at the sides of the tube could be bigger than calculated by the model. This would also worsen the heat transfer. In the model the curvature of the tube wall and surface tension effects are neglected.

In the inclined tube the film thickness is not axisymmetric and consequently there exists a circumferential temperature gradient with the highest temperature at the uppermost part of the tube. In the model it is assumed that the temperature at the inner tube wall is uniform. This simplifying assumption could also be a reason for the deviation between the theoretical values and the experimental ones.

According to the model the mean heat transfer coefficient at an inclination angle of 30° is about 5% larger than at an inclination angle of 45° (see Table 1). According to the experimental investigation the optimum inclination angle for the heat transfer is close to 40° (see Fig. 7b). However, for the majority of data points this deviation is in the range of the experimental uncertainty that was estimated to be 15% (refer to [14]). Hence it can be stated that there is a good agreement between the calculation and the experiment.

The optimum inclination angle for the flooding point was found to be between 45° and 60° (see Fig. [9]). Therefore for the investigated tube an inclination angle of about 45° is optimal with regard to the heat transfer as well as the flooding point.

Fig. 9b shows a comparison between experimental and theoretical data according to the model for the thickness of the condensate layer at the lowermost point of the tube. "Bottom" denotes a film thickness measurement at the position $z = 476$ mm and "top" a measurement at the position $z = 171$ mm (see [19]). The theoretical and the experimental film thicknesses are in good agreement. Except for a few data points the deviation between calculation and experiment is less than 15%.

5. Conclusions

It has been found that the inclination angle has a significant effect on the flooding point as well as on the heat transfer coefficient during reflux condensation of R134a. The optimum inclination angle at which the highest flooding vapour velocity occurs is between 45° and 60°. The optimum inclination angle for the heat transfer was found to be close to 40°. At this inclination angle the heat transfer is increased by a factor of nearly 2 when compared with reflux condensation in a vertical

tube. The reason for this significant increase is the non-uniform condensate distribution in an inclined tube. The analytical results for the film thickness and the mean heat transfer coefficient that were obtained by the presented model are in good agreement with the experimental data. The deviation is less than 15%.

Acknowledgements

It is gratefully acknowledged that financial support for this work has been provided in part by the Deutsche Forschungsgemeinschaft (DFG) (Au 67/15-1). Solvay Flour und Derivate GmbH is thanked for supplying the test fluid R134a.

References

[1] A.A. Mouza, S.V. Paras, A.J. Karabelas, Visual observations of flooding in inclined small diameter tubes, in: Proc. 3rd Europ. Thermal Sciences Conf., Heidelberg, Germany, 2000, pp. 1041–1046.

[2] G. English, W.T. Jones, R.C. Spillers, V. Orr, Flooding in a vertical updraft partial condenser, Chem. Eng. Progress 59 (1963) 51–53.

[3] ESDU Data Item No. 89038, Reflux condensation in vertical tubes, Heat Transfer Sub-series, vol. 6, 1989.

[4] W. Nusselt, Die Oberflächenkondensation des Wasserdampfes, VDI-Zeitschr. 60 (27) (1916) 541–546, and 60 (28) (1916) 568–578.

[5] S.S. Kutateladze, Fundamentals of Heat Transfer, Academic Press, New York, 1963.

[6] D.A. Labuntsov, Heat transfer in film condensation of pure steam on vertical surfaces and horizontal tubes, Teploenergetica 4 (1957) 72–80.

[7] J.C.Y. Wang, Y. Ma, Condensation heat transfer inside vertical and inclined thermosyphons, J. Heat Transfer 113 (1991) 777–780.

[8] K.-E. Hassan, M. Jakob, Laminar film condensation of pure saturated vapor on inclined circular cylinders, J. Heat Transfer 80 (1958) 887–894.

[9] J. Fürst, Kondensation in geneigten ovalen Rohren, Fortschr.-Ber. VDI, Reihe 19, Nr. 36, VDI-Verlag, Düsseldorf, 1989.

[10] G.P. Fieg, W. Roetzel, Calculation of laminar film condensation in/on inclined elliptical tubes, Int. J. Heat Mass Transfer 37 (1994) 619–624.

[11] G.P. Fieg, Laminare Filmkondensation an geneigten elliptischen Rohren unter dem Einfluss von Schwerkraft und Oberflächenspannung, Fortschr.-Ber. VDI, Reihe 19 (7), VDI-Verlag, Düsseldorf, 1986.

[12] S. Fiedler, S. Yildiz, H. Auracher, Determination of film thickness and flooding during reflux condensation in a small, inclined tube with an ultrasonic transducer, Int. J. Energy Res. 27 (4) (2003) 315–325.

[13] S. Fiedler, H. Auracher, Pressure drop during reflux condensation of R134a in a small diameter tube, in: Proc. Int. Symp. Compact Heat Exchangers, Grenoble, France, 2002, pp. 369–373.

[14] S. Fiedler, Untersuchungen zur Rücklaufkondensation in einem engen geneigten Rohr, Fortschr.-Ber. VDI, Reihe 3, Nr. 777, VDI-Verlag, Düsseldorf, 2003.

[15] D. Moalem Maron, S. Sideman, Condensation inside near horizontal tubes in co-current and counter-current flow, Int. J. Heat Mass Transfer 25 (1982) 1439–1444.

[16] K.W. McQuillan, P.B. Whalley, A comparison between flooding correlations and experimental flooding data for gas–liquid flow in vertical circular tubes, Chem. Eng. Sci. 40 (1985) 1425–1440.

[17] A. Zapke, D.G. Kröger, Countercurrent gas–liquid flow in inclined and vertical ducts—I: flow patterns, pressure drop characteristics and flooding, Int. J. Multiphase Flow 26 (2000) 1439–1455.

[18] A. Zapke, D.G. Kröger, Countercurrent gas–liquid flow in inclined and vertical ducts—II: the validity of the Froude–Ohnesorge number correlation for flooding, Int. J. Multiphase Flow 26 (2000) 1457–1468.

[19] S. Fiedler, C. Lohrer, H. Auracher, Experimental investigation and prediction of flooding during reflux condensation in a small diameter inclined tube, in: Proc. 12th Int. Heat Transfer Conf., Grenoble, France, 2002, pp. 303–308.

[20] W. Chen, Fluten bei Gegenstromkondensation in geneigten Rohren, Ph.D. thesis, Universität der Bundeswehr Hamburg, Germany, 1998.

[21] S. Fiedler, H. Auracher, D. Winkelmann, Effect of inclination on flooding and heat transfer during reflux condensation in a small diameter tube, Int. Comm. Heat Mass Transfer 29 (3) (2002) 289–302.

[22] S. Fiedler, B. Thonon, H. Auracher, Flooding in small-scale passages, Exp. Thermal Fluid Sci. 26 (2002) 525–533.